



Synthesis and spectroscopic characterization of new phthalocyanine derivatives: application as photocatalysts for the degradation of Orange G

Yusuf YILMAZ¹ , Kayode SANUSI^{2,*} ¹Naci Topçuoğlu Vocational School, Gaziantep University, Gaziantep, Turkey²Department of Chemistry, Obafemi Awolowo University, Ile-Ife, Nigeria

Received: 22.01.2019

Accepted/Published Online: 25.04.2019

Final Version: 06.08.2019

Abstract: New derivatives of 2(3),9(10),16(17),23(24)-tetrakis-(6-methylpyridin-2-yloxy)phthalocyanine (Pc) (**2b**, **2c**, and **2d**) were synthesized and their structures were characterized by elemental analysis, IR, ¹H NMR, and high-resolution mass spectrometry. The spectral results were in line with the proposed structures. The photodegradation of Orange G (OG) dye in DMSO by the Pc derivatives was investigated. The compounds showed relatively high photodegradation rates that increased with increasing size of the central atoms. The Pc photodegradation rates showed fair correlation with the singlet oxygen generation efficiencies (Φ_{Δ}). The observed rate constants were higher than the values already reported for other Pcs in the literature for the photodegradation of OG in aqueous media.

Key words: Photocatalysis, degradation, phthalocyanines, Orange G

1. Introduction

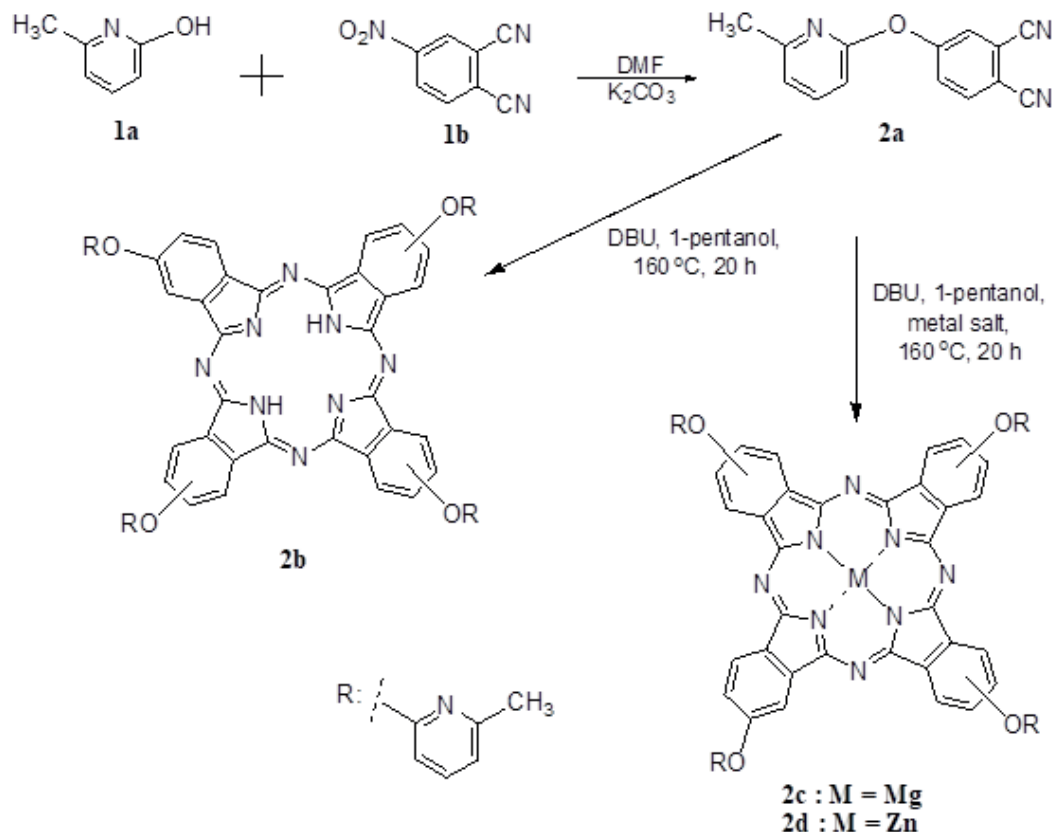
Over the years, there has been continued interest in the development of efficient photocatalysts for the removal of organic pollutants from water [1–5]. The process constitutes a means of removing persistent water contaminants such as dyes, which have high chemical stability and low biodegradability, via photocatalytic degradation [1–5]. In recent times, several techniques to improve the efficiency and reusability of the photoactive compounds responsible for photodegradation have been explored [6–9]. Some of such techniques include the development of photosensitizers supported on polymer matrices [6,7] and nanoparticles [8,9]. A promising candidate among the many previously tested compounds is the metallophthalocyanines (MPcs) [6–12]. This family of compounds is favored due to their excellent absorption in the visible range of the electromagnetic spectrum, their high chemical and thermal stability, and their remarkable ability to generate reactive singlet oxygen (¹O₂) from ground state molecular oxygen during photoexcitation [8,9,12].

Phthalocyanines (Pcs) and their derivatives have played important roles especially in the last 20–30 years in materials design [13–17]. As a result, many researchers have embarked on the synthesis of variously substituted Pcs aimed at obtaining new functional materials and molecular devices [13–17]. The ease of substitution around the Pc macrocycle and the flexibility of incorporating different metals into their central core make possible the actualization of this goal [13–17].

Since the ultimate goal of many researchers in this field is to obtain new photosensitizers with improved photoactivity, the focus of the present work was directed towards preparing new sets of Pcs (see Scheme below)

*Correspondence: sosanusi@oauife.edu.ng

with their full spectroscopic characteristics, and determining their singlet oxygen generation efficiencies (Φ_{Δ}) using a typical diphenylisobenzofuran (DPBF) degradation method [9,18]. Singlet oxygen has been shown to be the active species responsible for the photooxidation of organic dyes or pollutants [6–9].



Scheme. Synthetic routes for the preparation of **2b**, **2c**, and **2d**.

In the current study, the substituent (6-methylpyridyl moiety) was carefully chosen to provide an electron-rich aromatic pyridyl donor that could enhance the photocatalytic activity of the entire macrocycle, while the central atoms Mg and Zn were chosen to ascertain if indeed it was singlet oxygen generation or fluorescence that was responsible for photodegradation. The ZnPc will generate a higher singlet oxygen than MgPc due to the heavy atom effect, whereas MgPc will be more fluorescent than ZnPc. Obtaining a higher photodegradation rate with ZnPc would indicate that singlet oxygen is the dominating material in the photocatalysis, while having a higher photodegradation rate with MgPc would suggest that emission of photons by fluorescence is the dominating factor in the photocatalysis. The metal-free H_2Pc was studied to serve as a control, since it is expected to produce the least amount of singlet oxygen.

The molecule employed for the photodegradation experiment in the present study was Orange G (OG). OG is an azo dye that when largely absorbed by the environment is capable of causing cancer in humans. Thus, the dye poses a great environmental threat as it is one of the most commonly used synthetic colorants in the textile and ink industries [19,20]. The photodegradation rates of the dye in the presence of the new Pcs were investigated. The results obtained showed that the new Pcs have higher photocatalytic effects than the Pcs reported in the literature for OG photodegradation [8,9].

2. Experimental

2.1. Materials

Magnesium chloride, 4-nitrophthalonitrile, 6-methylpyridin-2-ol, potassium carbonate, zinc acetate ($\text{Zn}(\text{OAc})_2$), 1.8-diazabicyclo[5.4.0]undec-7-ene (DBU), zinc phthalocyanine (ZnPc), 1-pentanol, 2,5-dihydroxybenzoic acid, and Orange-G were purchased from Sigma-Aldrich. Dimethylformamide (DMF), dimethylsulfoxide (DMSO), methanol, ethanol, chloroform, acetone, CDCl_3 , $\text{DMSO}-d_6$, and Silica gel 60 used for column chromatography were obtained from Merck.

2.2. Equipment

Infrared (FT-IR) spectra were recorded on a PerkinElmer Spectrum 100 FT-IR spectrometer. Ground state electronic absorption spectra and photocatalytic procedures were performed on a Shimadzu UV-2550 spectrophotometer. ^1H NMR spectra were obtained using a Bruker Avance II 400 MHz spectrometer in $\text{DMSO}-d_6$ with tetramethylsilane (TMS) as reference. Mass spectra were collected on a Bruker Microflex LT MALDI-TOF-MS spectrometer. Elemental analyses were conducted using a Thermo Flash EA 2000 CHNS analyzer. Photoirradiation experiments were performed using a general electric quartz line lamp (300 W) with a 600-nm glass cut-off filter (Schott) and a water filter to filter off ultraviolet and infrared radiation, respectively. An interference filter (Intor, 700 nm with a band width of 40 nm) was additionally placed in the light path before the sample.

2.3. Synthesis

2.3.1. 4-(6-methylpyridin-2-yloxy)phthalonitrile (2a)

A mixture of 6-methylpyridin-2-ol, **1a**, (1.30 g, 11.9 mmol) and 4-nitrophthalonitrile, **1b**, (1.00 g, 5.78 mmol) was vigorously stirred in 10 mL of dry DMF for 15 min. Thereafter, finely ground anhydrous K_2CO_3 (1.54 g, 11.2 mmol) was added to the mixture portionwise within 2 h. The reaction mixture was continuously stirred with the temperature increased to 45 °C under nitrogen for 20 h. At completion, the mixture was poured into 100 mL of ice water for precipitation, after which it was filtered off to collect the precipitate. The product was recrystallized from a mixture of ethanol/water (100:1). Yield: (72%). mp = 120–121 °C. IR [ATR] ($\nu_{\text{max}}/\text{cm}^{-1}$): 3109–2999 (Ar. -H), 2966–2842 (Aliph. -CH), 2232 ($-\text{C}\equiv\text{N}$) 1563 (Ar. $-\text{C}=\text{C}$), 1243 (C–O–C). ^1H NMR (400 MHz, $\text{DMSO}-d_6$, δ , ppm): 8.16–6.44 (6H, m, Ar. -H), 2.36 (3H, s, C–H). MS (MALDI TOF) m/z : Calcd 235; found: 236 $[\text{M} + \text{H}]^+$. CHN Anal. Calcd for $\text{C}_{14}\text{H}_9\text{N}_3\text{O}$ (%): C, 71.48; H, 3.86; N, 17.8. Found (%): C, 70.54; H, 3.53; N, 16.30.

2.3.2. 2(3),9(10),16(17),23(24)-Tetrakis-(6-methylpyridin-2-yloxy)phthalocyanine (2b)

The phthalonitrile **2a** (100 mg, 0.43 mmol) was dissolved in 5 mL of 1-pentanol, heated to 110 °C under nitrogen with vigorous stirring, and a catalytic amount of DBU (10 μL) was added. Thereafter, the temperature of the reaction mixture was raised to 160 °C and left to stir for 20 h. The crude product was cooled and washed in 20 mL of methanol. The precipitate formed was washed again several times in methanol and water. The yellowish green solid was dried in air and ground into a powder before further purification. The final purification was achieved by column chromatography with silica gel as the stationary phase and chloroform/methanol (9:1) as the mobile phase.

Compound **2b** yield: (16%). mp > 300 °C. UV-vis. (DMSO)- λ_{max} (nm), (log e): 669 (5.30), 710 (5.30). IR [ATR] (ν_{max}/cm^{-1}): 3250 (–NH), 3080 (Ar. –H), 2952–2860 (Aliph. –CH), 1536 (Ar. –C=C), 1180 (–C–O–C–). ^1H NMR (400 MHz, DMSO- d_6 , δ , ppm): 7.85–7.13 (24H, m, Ar. –H), 2.46–2.34 (12H, m, C–H). MS (MALDI TOF) m/z : Calcd 943; found 944 $[\text{M} + \text{H}]^+$. CHN Anal. Calcd for $\text{C}_{56}\text{H}_{38}\text{N}_{12}\text{O}_4$ (%): C, 71.33; H, 4.06; N, 17.82. Found (%): C, 70.55; H, 4.12; N, 16.95.

2.3.3. 2(3),9(10),16(17),23(24)-Tetrakis-(6-methylpyridin-2-yloxy)phthalocyaninato magnesium (2c) or zinc(II) (2d) complex

The synthesis and purification of **2c** and **2d** were similar except that 19 mg (0.20 mmol) of magnesium chloride was employed as the metal salt for **2c** and 38 mg (0.21 mmol) of zinc(II) acetate was used for **2d**. The metal salt (MgCl_2 or zinc acetate) and 100 mg of **2a** were dissolved in 5 mL of 1-pentanol. The mixture was heated to 110 °C under nitrogen atmosphere while being stirred vigorously. A catalytic amount of DBU (10 μL) was added at this point and the temperature of the mixture was raised to 160 °C with continued stirring for 20 h. The crude product was thereafter cooled to room temperature and washed in 20 mL of methanol. The precipitate formed was washed again several times in methanol and water. The yellowish green solid was dried in air and ground into a powder before further purification. The final purification was achieved by column chromatography using silica gel as the stationary phase and chloroform/methanol (9:1) as the mobile phase.

Complex **2c** yield: (20%), mp > 300 °C. UV-vis. (DMSO)- λ_{max} (nm), (log e): 670 (5.33), 608 (4.55), 345 (4.80). IR [ATR] (ν_{max}/cm^{-1}): 3072 (Ar. –H), 2925–2833 (Aliph.-CH), 1524 (Ar. –C=C), 1240 (C–O–C). ^1H NMR (400 MHz, DMSO- d_6 , δ , ppm): 7.85–7.13 (24H, m, Ar. –H), 2.46–2.34 (12H, m, C–H). MS (MALDI TOF) m/z : Calcd 965; found: 965 $[\text{M}]^+$. CHN Anal. Calcd for $\text{C}_{56}\text{H}_{36}\text{N}_{12}\text{O}_4\text{Mg}$ (%): C, 69.68; H, 3.76; N, 17.41. Found (%): C, 69.52; H, 3.45; N, 16.98.

Complex **2d** yield: (25%), mp > 300 °C. UV-vis. (DMSO)- λ_{max} (nm), (log e): 680 (5.35), 610 (4.83), 347 (4.92). IR [ATR] (ν_{max}/cm^{-1}): 3050 (Ar. –H), 2972–2826 (Aliph. –CH), 1570 (Ar. –C=C), 1223 (C–O–C). ^1H NMR (400 MHz, DMSO- d_6 , δ , ppm): 7.85–7.13 (24H, m, Ar. –H), 2.46–2.34 (12H, m, C–H). MS (MALDI TOF) m/z : Calcd 1006; found: 1007 $[\text{M} + \text{H}]^+$. CHN Anal. Calcd for $\text{C}_{56}\text{H}_{36}\text{N}_{12}\text{O}_4\text{Zn}$ (%): C, 66.84; H, 3.61; N, 16.70. Found (%): C, 66.70; H, 3.75; N, 15.95.

2.4. Singlet oxygen quantum yield determination

The singlet oxygen ($^1\text{O}_2$) quantum yields Φ_{Δ} for **2b**, **2c**, and **2d** were determined using the literature method [9,18,21] and applying the following equation:

$$\Phi_{\Delta} = \Phi_{\Delta}^{Std} \frac{R \times I_{abs}^{std}}{R^{std} \times I_{abs}}$$

where Φ_{Δ}^{Std} is the singlet oxygen quantum yield of the standard ZnPc, and R and R^{std} are the photodegradation rates of the singlet oxygen quencher DPBF in the presence of the samples (**2b**, **2c**, and **2d**) and the standard, respectively. I_{abs} and I_{abs}^{std} are the rates of light absorption by the samples and standard, respectively [9,18,21].

3. Results and discussion

3.1. Synthesis and characterization

The spectroscopic data of the new compounds were satisfactory and consistent with the predicted structures as shown in the Scheme. The compounds were characterized with UV-visible spectrophotometry, MALDI-TOF MS, IR, ^1H NMR, and elemental spectroscopic techniques. The band at 1243 cm^{-1} was ascribed to the $-\text{C}-\text{O}-\text{C}-$ vibration of compound **2a**, suggesting its successful formation. The multiplets observed in the ^1H NMR spectrum at 8.16–6.44 and the singlet peak at 2.36 ppm were attributed to the magnetic resonance of the 6 aromatic and the 3 methyl protons, respectively. The peak at $m/z = 236$ found in the MALDI-TOF MS spectrum of **2a** is equivalent to a molecular ion peak $[\text{M} + \text{H}]^+$, which confirmed its successful formation (Figure 1). The nitrile ($-\text{C}\equiv\text{N}$) band at 2232 cm^{-1} in compound **2a** disappeared upon cyclization to the respective Pcs (**2b**, **2c**, and **2d**), (Figure 2, showing **2d** as a representative sample). The bands at 3250 and 1536 cm^{-1} are consistent with typical vibrational stretching and bending modes, respectively, of the secondary amines [22] found in **2b**, suggesting the presence of the core secondary amine ($-\text{NH}$) in the target compound after cyclization. The ^1H NMR spectra of the Pcs in deuterated DMSO showed 24 proton multiplets upon integration, and they are attributed to the Ar. $-\text{H}$ protons at 7.85–7.13 ppm. The nonobservance of inner NH protons is common in metal-free Pcs, and the reason has been attributed to the aggregation effect [23]. The mass spectra data were collected on a Bruker Microflex LT MALDI-TOF-MS spectrometer using 2,5-dihydroxybenzoic acid as the matrix in positive ion mode. The MS peaks at $m/z = 944$, 965 , and 1007 correspond to the molecular ions $[\text{M} + \text{H}]^+$, $[\text{M}]^+$, and $[\text{M} + \text{H}]^+$ of **2b**, **2c**, and **2d**, respectively (Figure 1 with **2d** as a representative sample). MPc complexes were observed to fragment with molecular ion peaks $[\text{M}]^+$, $[\text{M} + n\text{H}]^+$, or $[\text{M} - n\text{H}]^+$ [24], hence confirming the correctness of the observed mass spectral data. The measured C, H, and N elemental data are consistent with the predicted structures, which confirms the purity of the target compounds. The UV-visible spectra of the compounds show the typical absorption bands for Pcs: the Q- and B-bands (Figure 3). The compounds showed high solubility in some of the common organic solvents tested, which include DMF, CHCl_3 , and THF, as no indication of aggregation resulting from decreased solubility was observed in the electronic absorption spectra in these solvents (Figure 4 with **2d** as a representative sample). Since they are tetrasubstituted derivatives, each Pc (**2b**, **2c**, or **2d**) contained a mixture of four positional isomers, which would have the following symmetry groups: D_{2h} , C_{4h} , C_{2v} , and C_s [23]. The high intense absorption observed for **2b** in the 300–400 nm region was attributed to the superimposition of the electronic absorption of the C_s isomer over the absorption of the other three isomers (D_{2h} , C_{4h} , and C_{2v}) (Figure 3).

3.2. Singlet oxygen quantum yields

The singlet oxygen quantum yields of the compounds were determined by spectrophotometric method with the use of a known singlet oxygen quencher, diphenylisobenzofuran (DPBF) in DMSO [9,18,21]. The singlet oxygen quantum yields (F_D) obtained for the compounds were 0.35, and 0.45 for **2b**, **2c**, and **2d**, respectively, implying that the F_D values increased from the H_2Pc to ZnPc in the order $\text{H}_2\text{Pc} < \text{MgPc} < \text{ZnPc}$. In similar work done in the past, some Pc molecules either unattached or as composites with polymer fibers or nanoparticles were reported to show considerably high F_D values in the range 0.32–0.59 in water or DMF [6,9], while many others showed remarkably low values [7,8] when compared to those obtained in the present work.

Figure 5 shows the degradation of DPBF upon irradiation in the presence of **2d** complex (as a representative) for a varying length of time. The decrease in DPBF absorbance was monitored at $\sim 417\text{ nm}$. There

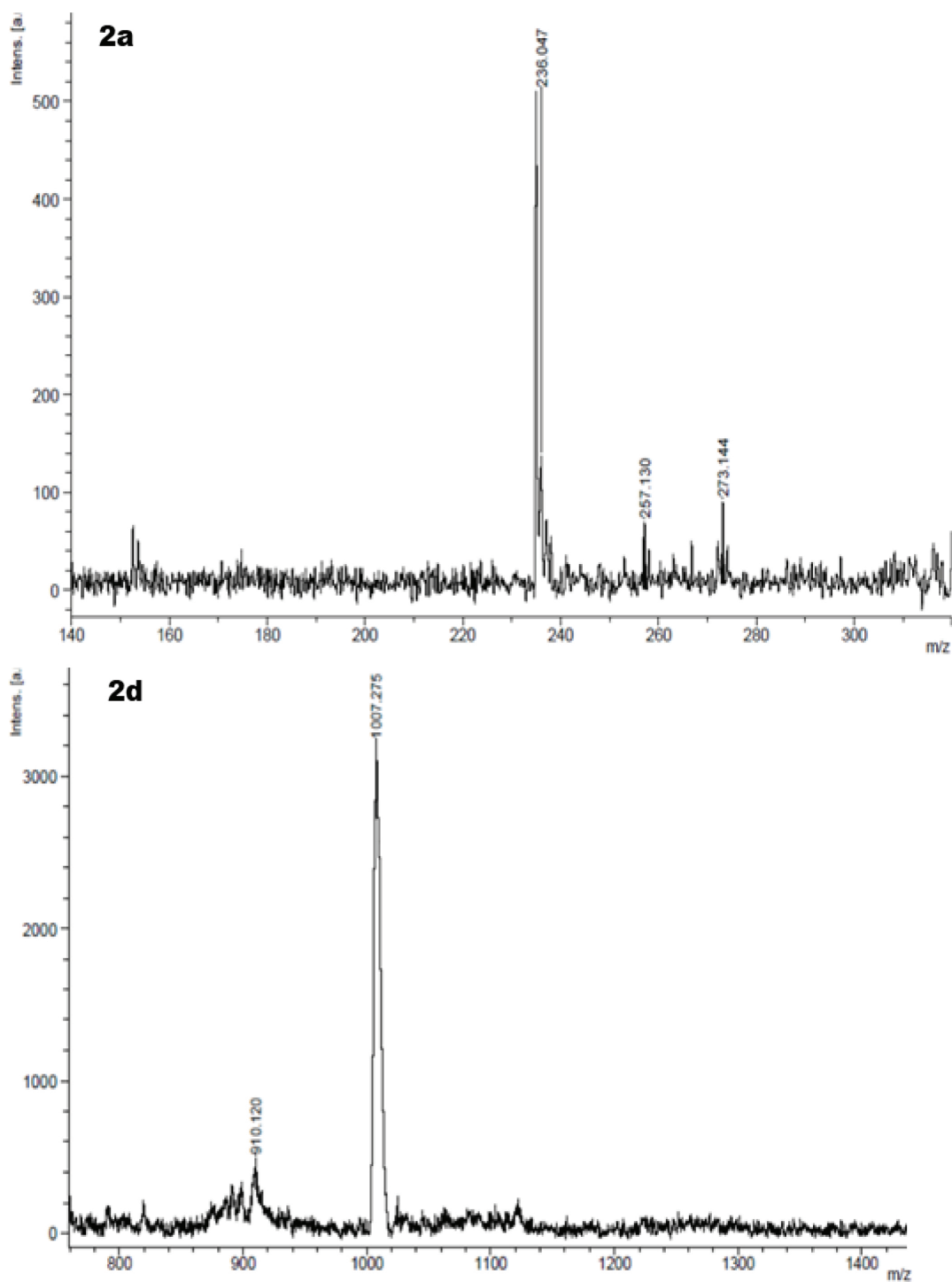


Figure 1. MALDI-TOF MS spectra of compounds **2a** and **2d**.

was no observed decrease in the absorbance of the Pc Q-band upon irradiation throughout the period of the experiment. Similar behaviors were observed for compounds **2b** and **2c**, suggesting that the Pcs were considerably photostable, and are therefore suitable for use as photocatalysts, and could also be considered for other

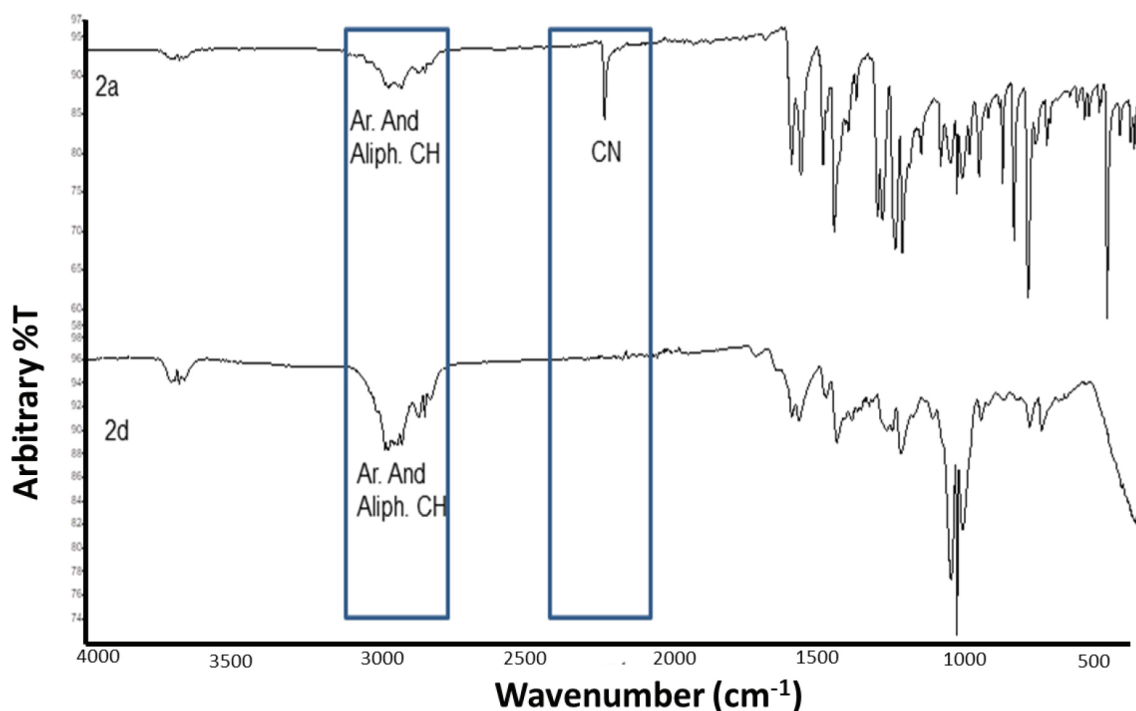


Figure 2. FT-IR spectra of compounds **2a** and **2d**.

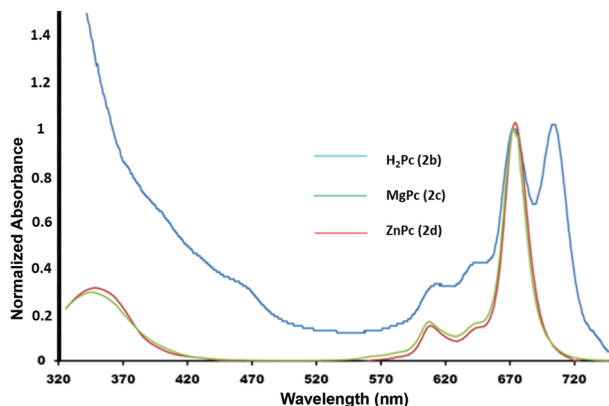


Figure 3. Ground state absorption spectra of **2b**, **2c**, and **2d** in DMSO. Conc. $\sim 5.00 \times 10^{-6}$ M.

applications in the photonics and optoelectronics fields that require molecules with sufficient stability under photon irradiation.

3.3. Photocatalytic degradation of Orange G

The absorption spectral changes of OG upon photoirradiation at 5-min intervals using **2d** as the photocatalyst are shown in Figure 6 (as a representative). The degradation was monitored by observing the change in the OG absorbance at 497 nm in DMSO. OG behavior upon photoirradiation in the absence of Pcs is also presented in Figure 7 for the purpose of comparison. The degree of degradation of the OG as caused by light in the absence of Pcs was insignificant (Figure 7) when compared to when Pcs were present (Figures 6). This suggests that the photodegradation of the pollutant was enhanced mainly by the Pcs.

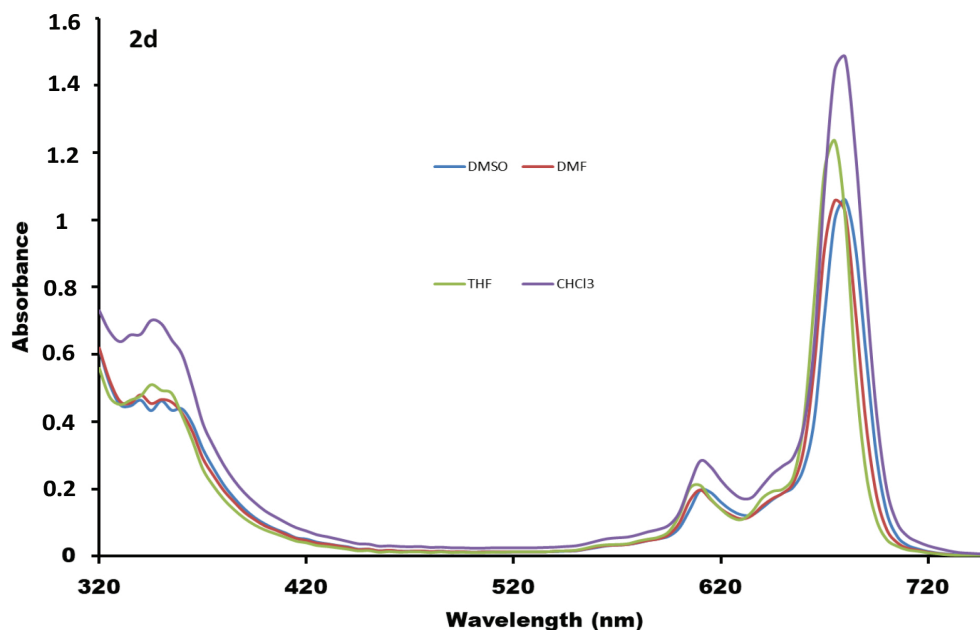


Figure 4. Absorption spectra of **2d** in different solvents (DMSO, DMF, THF, and CHCl_3). Conc. $\sim 1.10 \times 10^{-5}$ M.

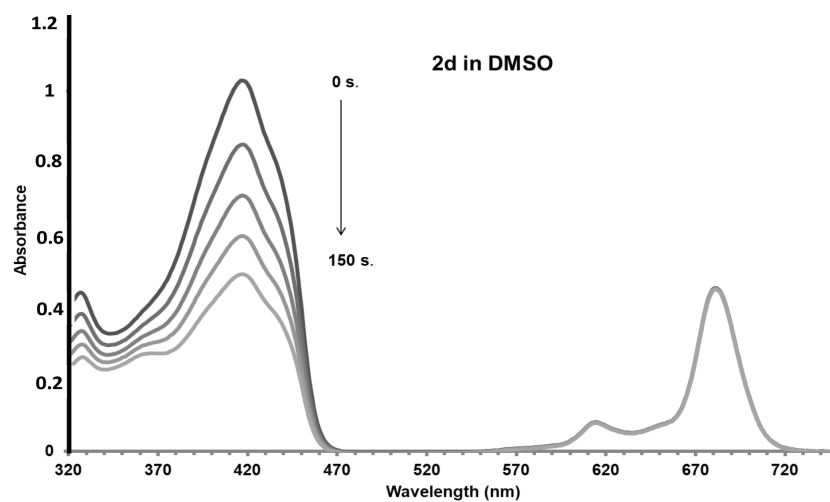


Figure 5. Changes in the absorbance of DPBF (1.5×10^{-5} M) in the presence of **2d** (0.5×10^{-5} M) for singlet oxygen quantum yield determination in DMSO.

It is noteworthy that previous work on the photodegradation of this dye was carried out in different aqueous media that have low Pc solubility [8,9,25,26]. We think that the photocatalytic degradation effect of Pcs fell due to the decreased solubility in aqueous media. A study of the degradation in DMSO would therefore better reveal the true photocatalytic property of Pcs in degrading OG dye.

In the present study, the concentration of OG employed in the presence of 9.0×10^{-6} M of each Pc was 2.5×10^{-4} M. This concentration (of OG) was significantly higher than those considered in the work reported by Ledwaba et al. [9], but slightly less than the amount reported by Modisha et al. [8] for Pcs alone.

The performances of the studied Pcs relative to those earlier reported [8,9] are presented in Table. The

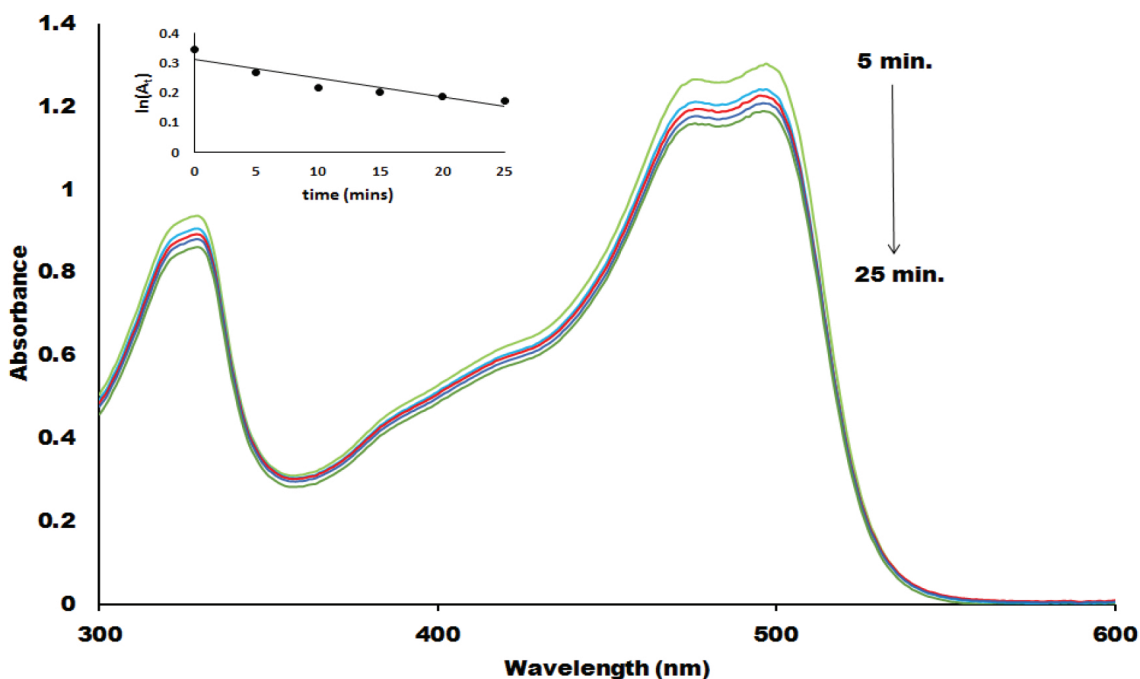


Figure 6. Photocatalytic degradation of 2.5×10^{-4} M OG in the presence of 9.0×10^{-6} M **2d** in DMSO (Inset: A plot of $\ln(A_t)$ of OG versus time).

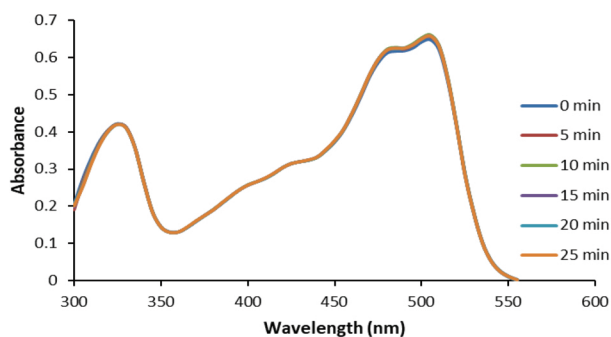


Figure 7. Photoirradiation of orange G (OG) in the absence of Pcs. Conc. of OG employed is $\sim 2.5 \times 10^{-6}$ M.

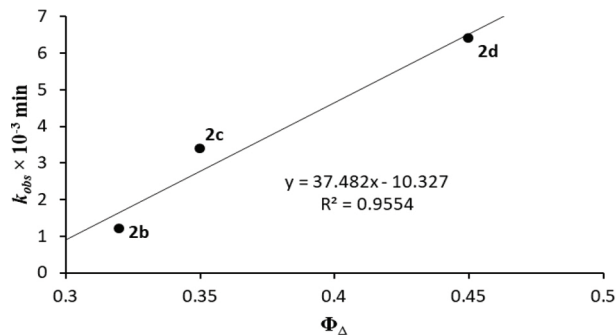


Figure 8. The observed relationship between photodegradation rate and singlet oxygen quantum yield.

observed rate constants (k_{obs}) for each Pc, **2b** ($1.2 \times 10^{-3} \text{ min}^{-1}$), **2c** ($3.4 \times 10^{-3} \text{ min}^{-1}$), and **2d** ($6.4 \times 10^{-3} \text{ min}^{-1}$) were considerably larger than those reported before in the literature [8,9] (Table), if the amounts of OG employed in these studies are put into perspective. In addition to the effect of Pc, it could be assumed that the solvent employed, which is DMSO, may play an important role in enhancing the photodegradation as well. Meanwhile, since the amounts of Pcs used in the previous works were not explicitly stated, it is difficult to unambiguously compare our results with the previous ones [8,9,25,25], thus making it impossible to identify if there were enhancements or not. Nevertheless, considering that the concentration of Pcs used in the present work was at the barest minimum, it could be safely concluded that the new Pcs in DMSO showed higher degradation rates than the previously reported Pcs in aqueous media [8,9]. In Figure 8, the photodegradation rates are shown to increase with increasing singlet oxygen quantum yield. It can be seen that the two parameters fairly correlate, with an R^2 value of 0.9554.

Table. Literature k_{obs} data for different concentrations of OG degraded in the presence of Pcs as compared to those obtained in the present work.

[OG] $\times 10^{-5}$ M	$k_{obs} \times 10^{-3}$ min $^{-1}$	Pcs employed	References
26.5	1.0	ZnOCPc	[8]
2.3	8.0	ZnTCPPc	[9]
3.5	5.8	ZnTCPPc	[9]
4.8	1.0	ZnTCPPc	[9]
25.0	1.2	2b	This work
25.0	3.4	2c	This work
25.0	6.4	2d	This work

ZnOCPc = zinc(II)octacarboxyphthalocyanine and ZnTCPPc = zinc(II)tetracarboxyphenoxyphthalocyanine

3.4. Conclusions

Overall, the spectroscopic characteristics of new sets of Pcs with moderate singlet oxygen quantum yield (Φ_{Δ}) values are reported. These Pcs were found to show considerably high photodegradation rates for the degradation of OG in DMSO when compared to some Pcs reported earlier in aqueous media. It was opined that, in addition to the enhanced photocatalytic effect of the Pcs (**2b**, **2c**, and **2d**), the solvent employed, that is DMSO, may also play an important role in increasing the photodegradation rates.

Acknowledgment

This research was partly supported by Gaziantep University (Project Number: FEF.YLT.17.01).

References

1. Suri RPS, Liu J, Hand DW, Crittenden JC, Perram DL et al. Heterogeneous photocatalytic oxidation of hazardous organic contaminant in water. *Water Environment Research* 1993; 65: 665-673.
2. Bhatkhande DS, Kamble SP, Sawant SB, Pangarkar VG. Photocatalytic and photochemical degradation of nitrobenzene using artificial UV radiation. *Chemical Engineering Journal* 2004; 102: 283-290.
3. Devipriya S, Yesodharan S. Photocatalytic degradation of pesticide contaminants in water. *Solar Energy Material and Solar Cell* 2005; 86: 309-348.
4. Mele G, del Sole R, Vasapollo G, Garcia-López E, Palmisano L et al. Photocatalytic degradation of 4-nitrophenol in aqueous suspension by using polycrystalline TiO₂ impregnated with functionalized Cu(II)-porphyrin or Cu(II)-phthalocyanine. *Journal of Catalysis* 2003; 217: 334-342.
5. Chatterjee D, Dasgupta S. Visible light induced photocatalytic degradation of organic pollutants. *Journal of Photochemistry and Photobiology C: Photochemistry Reviews* 2005; 6: 186-205.
6. Zügler R, Nyokong T. Zinc(II) 2,9,16,23-tetrakis[4-(N-methylpyridyloxy)]-phthalocyanine anchored on an electrospun polysulfone polymer fiber: application for photosensitized conversion of methyl orange. *Journal of Molecular Catalysis A: Chemical* 2013; 366: 247-253.
7. Zügler R, Antunes E, Khene S, Nyokong T. Photooxidation of 4-chlorophenol sensitized by lutetium tetraphenoxy phthalocyanine anchored on electrospun polystyrene polymer fiber. *Polyhedron* 2012; 33: 74-81.
8. Modisha P, Nyokong T, Antunes E. Photodegradation of Orange G using zinc octacarboxyphthalocyanine supported on Fe₃O₄ nanoparticles. *Journal of Molecular Catalysis A: Chemical* 2013; 380: 131-138.

9. Ledwaba M, Masilela N, Nyokong T, Antunes E. Surface modification of silica-coated gadolinium oxide nanoparticles with zinc tetracarboxyphenoxy phthalocyanine for the photodegradation of Orange G. *Journal of Molecular Catalysis A: Chemical* 2015; 403: 64-76.
10. Fernández L, Esteves VI, Cunha Â, Schneider RJ, Tomé JPC. Photodegradation of organic pollutants in water by immobilized porphyrins and phthalocyanines. *Journal of Porphyrins and Phthalocyanines* 2016; 20: 150-166.
11. Mahmiani Y, Sevim AM, Gül A. Photocatalytic degradation of persistent organic pollutants under visible irradiation by TiO₂ catalysts sensitized with Zn(II) and Co(II) tetracarboxy-phthalocyanines. *Journal of Porphyrins and Phthalocyanines* 2016; 20: 1190-1199.
12. Nyokong T, Antunes E. Photochemical and photophysical properties of metallophthalocyanines. In: Kadish KM, Smith KM, Guillard R (editors). *The Handbook of Porphyrin Science*. Vol. 7. New York, NY, USA: Academic Press, 2010, pp. 247-349.
13. Sanusi K, Antunes E, Nyokong T. Optical nonlinearities in non-peripherally substituted pyridyloxy phthalocyanines: a combined effect of symmetry, ring-strain and demetallation. *Dalton Transactions* 2014; 43: 999-1010.
14. Yoshida T, Tochimoto M, Schlettwein D, Wöhrle D, Sugiura T et al. Self-assembly of zinc oxide thin films modified with tetrasulfonated metallophthalocyanines by one-step electrodeposition. *Chemistry of Materials* 1999; 11: 2657-2667.
15. Rosenthal I. Phthalocyanines as photodynamic sensitizers. *Photochemistry and Photobiology* 1991; 53: 859-870.
16. Osifeko OL, Nyokong T. Applications of lead phthalocyanines embedded in electrospun fibers for the photoinactivation of *Escherichia coli* in water. *Dyes and Pigments* 2014; 111: 8-15.
17. Adegoke O, Nyokong T. Fluorescence "turn on" probe for bromide ion using nanoconjugates of glutathione-capped CdTe@ZnS quantum dots with nickel tetraamino-phthalocyanine: characterization and size-dependent properties. *Journal of Photochemistry and Photobiology A: Chemistry* 2013; 265: 58-66.
18. Ogunsipe A, Chen JY, Nyokong T. Photophysical and photochemical studies of zinc(II) phthalocyanine derivatives-effects of substituents and solvents. *New Journal of Chemistry* 2004; 28: 822-827.
19. Daneshvar N, Salari D, Khataee AR. Photocatalytic degradation of azo dye acid red 14 in water on ZnO as an alternative catalyst to TiO₂. *Journal of Photochemistry and Photobiology A: Chemistry* 2003; 157: 111-116.
20. Lachheb H, Puzenat E, Houas A, Ksibi M, Elaoui E et al. Photocatalytic degradation of various types of dyes (Alizarin S, Crocein Orange G, Methyl Red, Congo Red, Methylene Blue) in water by UV-irradiated titania. *Applied Catalysis B: Environmental* 2002; 39: 75-90.
21. Ogunsipe A, Maree D, Nyokong T. Solvent effects on the photochemical and fluorescence properties of zinc phthalocyanine derivatives. *Journal of Molecular Structure* 2003; 650: 131-140.
22. Coates J. Interpretation of infrared spectra: a practical application approach. In: Meyers RA (editor). *Encyclopedia of Analytical Chemistry*. Chichester, West Sussex, UK: John Wiley & Sons Ltd, 2000, pp. 10815-10837.
23. Gounden D, Ngubeni GN, Louzada MS, Khene S, Britton J et al. Synthesis, spectroscopic and DFT characterization of 4β-(4-*tert*-Butylphenoxy)phthalocyanine positional isomers for non-linear optical absorption. *South African Journal of Chemistry* 2017; 70: 49-59.
24. Tolbin AY, Pushkarev VE, Nikitin GF, Tomilova LG. Heteroligand and heteronuclear clamshell-type phthalocyanines: selective preparation, spectral properties, and synthetic application. *Tetrahedron Letters* 2009; 69: 4848-4850.
25. Chauke V, Nyokong T. Photocatalytic oxidation of 1-hexene using GaPc and InPc octasubstituted derivatives. *Journal of Molecular Catalysis A: Chemical* 2008; 289: 9-13.
26. Modisha P, Nyokong T. Fabrication of phthalocyanine-magnetic nanoparticles hybrid nanofibers for degradation of Orange-G. *Journal of Molecular Catalysis A: Chemical* 2014; 381: 132-137.